

An experimental investigation of supercritical CO₂ accidental release from a pressurised pipeline

Kang Li¹, Xuejin Zhou¹, Ran Tu², Qiyuan Xie¹, Jianxin Yi¹ and Xi Jiang^{3*}

¹ Department of Safety Science Engineering & State Key Laboratory of Fire Science, University of Science and Technology of China, Hefei, Anhui 230026, China

² College of Mechanical Engineering and Automation, Huaqiao University, Jimei, Xiamen 361000, China

³ Engineering Department, Lancaster University, Lancaster LA1 4YR, UK

* Corresponding author. E-mail: x.jiang@lancaster.ac.uk; Tel: (+44) 1524 592439

ABSTRACT

Experiments at laboratory scales have been conducted to investigate the behaviour of the release of supercritical CO₂ from pipelines including the rapid depressurization process and jet flow phenomena at different sizes of the leakage nozzle. The dry ice bank formed near the leakage nozzle is affected by the size of the leakage nozzle. The local Nusselt numbers at the leakage nozzle are calculated and the data indicate enhanced convective heat transfer for larger leakage holes. The mass outflow rates for different sizes of leakage holes are obtained and compared with two typical accidental gas release mathematical models. The results show that the “hole model” has a better prediction than the “modified model” for small leakage holes. The experiments provide fundamental data for the CO₂ supercritical-gas multiphase flows in the leakage process, which can be used to guide the development of the leakage detection technology and risk assessment for the CO₂ pipeline transportation.

Highlights:

- Dry ice bank is formed near the leakage hole for the nozzle of medium size;
- The Mach number indicates a change from sonic to subsonic leakage of the supercritical CO₂;
- The heat transfer at the leakage nozzle is enhanced with increasing leakage nozzle size.
- The “hole model” predicts the mass outflow rate better than the “modified model” for small leakage holes.

KEYWORDS: supercritical CO₂ accidental release, carbon capture and storage, choked flow, Mach number, Nusselt number, pipeline transportation.

1. Introduction

To meet the challenges in the transition period between the current fossil fuel based economy and a future renewable and sustainable technological era, carbon capture and storage (CCS) is considered as one of the major options for the mitigation of CO₂ emissions from the power generation plants and other carbon-intensive sources. The CCS technologies have obtained increasing global interests in the last decades [1-5]. As one of the three main parts in the CCS chain, transportation of CO₂ from capture plants to storage sites requires a reliable and elaborate transportation system. Previous studies have identified pipeline as the most economical method for transporting large amounts of CO₂. As the dominant mode for transportation of CO₂, pipeline transportation system is not a new technology [6-9]. The majorities of the CO₂ pipelines are located in North America with over 30 years of experience in carrying CO₂ [10]. Compared with the natural gas pipeline transportation system, CO₂ pipeline transportation system has a shorter operating history and most existing CO₂

pipelines are settled in remote areas. CO₂ pipelines require similar materials as those for natural gas pipelines [11], but there are important differences. Considering the service life of pipelines, the internal corrosion during the fatigue life of the pipeline needs to be taken into account in the operation of the pipeline transportation system [12]. Corrosion could be caused by the possible water content in the transported CO₂. Potential leakage can take place with the development of corrosion and small cracks might develop near the valves or the fitting joints. Leakage detection technology and risk assessment of the accidental release of CO₂ provide assurance for the effective operation of the pipelines and for the surrounding environments, especially when increasing CO₂ pipeline transportation systems have to be built and settled in less remote areas. The leaked CO₂ would accumulate in local areas which might cause asphyxia endangering safety of human beings and animals around if it accumulates to a high concentration [13]. As the property of CO₂ transported is quite different from natural gas, several complex phenomena occur during the leakage process [14, 15]. In order to provide fundamental knowledge on the leakage process for the development of technologies to address the safety concern of the pipeline transportation system and concerns on the surrounding environments including human activities, an experimental investigation of the behaviour of supercritical CO₂ release under laboratory conditions was conducted in this study.

Pipelines of the CO₂ transportation could be categorized into different types of systems: the gathering system, the main pipeline system, and the distribution system. The gathering system transports the dry, low-pressure CO₂ from capture plants to compression stations, often using small diameter pipelines; the main pipeline system takes the CO₂ after compression and transports the high pressure CO₂ along the transportation route, and the distribution system transports CO₂ from the main pipeline system to the storage sites. CO₂ is generally transported in the main pipeline system at pressure and temperature ranged from 8.5 MPa to 15 MPa and 12 °C to 44 °C, respectively. The lower pressure and temperature limits are set by the phase behavior of CO₂ so that it can be maintained at supercritical

condition which is the most economical way for transportation [9]. The main pipeline system consists of pipelines, compressor stations, metering stations, valves, control stations, supervisory control and data acquisition (SCADA), and pigs. CO₂ is compressed in the compressor stations so that it is kept in supercritical phase along the pipelines. Metering stations, valves, control stations and SCADA are the monitor and controller of the pipelines in the CO₂ pipeline transportation system. Pigs are sophisticated robotic devices used for inspection of the pipelines for corrosion and detection of defects to ensure the efficient and safe operation of the extensive network of pipelines. As most of the CO₂ transportation pipelines are still in service life, CO₂ transportation systems have not been fully tested in last decades and the amount of available data is rather limited. According to a survey of accidents for pipeline transportation system, most of unintentional release of CO₂ occurred in the main pipelines [16]. The most frequent causes of the accidents are external interference, corrosion, construction defect, and ground movement [17]. In the analysis of such accidents, the first stage is to estimate the mass outflow rate at which the gas is being released through the damaged pipe [16, 18]. It is actually a complex problem which begins with the “hole diameter” definition where a particular opening size needs to be assumed: “rupture”, “hole”, and “pinhole” are the three main “hole diameter” sizes used to define the opening size in natural gas pipelines. In general, “rupture” refers the whole cross section of the pipeline is completely broken, while “hole” is the opening size whose diameter is larger than 20 mm (widely used in natural gas accident analysis) and “pinhole” refers to sizes that are smaller than 20 mm [17]. Estimating the mass outflow rate of CO₂ released from damaged pipeline can be performed mainly using two models: the “hole model” and “pipe model” [16]. The “hole model” is used for release at “pinhole” while “pipe model” for the release at “rupture”. Nevertheless neither of these models could well satisfy the leakage hole between “pinhole” and “rupture”, a new modified model was proposed by Dong et al. [19, 20], which is used to bridge the gap between the “hole model” and “pipe model” and referred to as the “modified model”. Since CO₂ is also highly pressurised as natural gas but their properties are quite

different, the parameters for measuring the accidental release of natural gas may not be suitable for CO₂. To analyze the accidental release of the highly pressurized CO₂, the leakage hole types need to be determined first in terms of the physical property of CO₂, and then the calculation of the mass outflow rate and the investigation of the depressurization process could follow.

In this study, experiments were setup to evaluate the CO₂ outflow from the leakage holes. The depressurization process and multiphase choked flow at the leakage nozzle with different leakage hole sizes were measured and the mass outflow rates were obtained, followed by comparisons of the experimental results with the typical accidental release model predictions. The study is focused on the flow characteristics of leakage process near the leakage nozzle instead of the plume entrainment downstream. In the following, a brief introduction of experiments is firstly presented, followed by experimental and computational results and their discussions. Finally, some conclusions from the study are drawn.

2. Experiments

2.1. Experimental setup

In the experiments, 5 different leakage nozzle sizes were used as the leakage hole ranging from small to relatively big holes. Ratio of hole diameter to pipe diameter (RHP) was chosen to characterise the leakage nozzle which is defined as:

$$RHP = d_e / D_p \quad (1)$$

where D_p is the diameter of the pipeline and d_e is the diameter of the hole which refers to the equivalent diameter of nozzle and could be calculated as follows:

$$d_e = \sqrt{4S / \pi} \quad (2)$$

where S is the area of the nozzle (leakage hole). The details of leakage nozzle are shown in

Fig. 1.

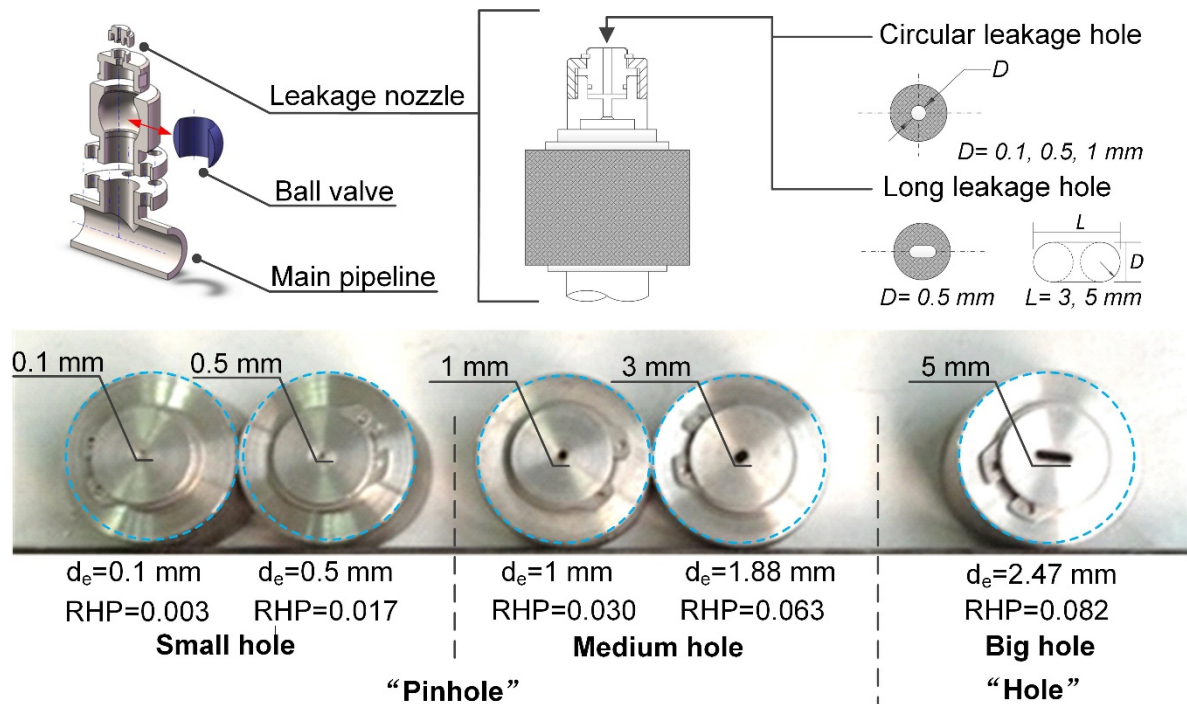


Fig. 1. Details of the leakage nozzle.

Generally, the pipelines operated in last decades in transportation systems have diameters of 250~300 mm [9]. According to the fact that the accidental release hole diameter of 20 mm is widely used in gas pipelines to divide “pinhole” and “hole”, RHP of 0.07 is chosen in this study to separate the “pinhole” from “hole”. As the behaviour of the pressurised CO₂ leakage is quite different when RHP<0.02, these types of accidental release holes are classified as small holes.

To investigate the leakage behaviour of supercritical CO₂ from pipeline, a recently developed in-house facility was used to study the accidentally leakage of CO₂ [21]. It consists of two main parts: the control panel and main pipeline. CO₂ from the gas cylinder was conditioned into supercritical phase through the control panel and then injected into the test section which was kept circulating in the main pipeline in the experiments. The test section is located in the main pipeline part to obtain the pressure and temperature data inside the pipeline during the leakage process. The main pipeline in the test section is made of steel tube with an inner

diameter of 30 mm and a length of 10 m. It is coated by heat band which keeps the CO₂ inside the pipeline at a constant temperature of 40 °C, and glass wool insulation which keeps the whole leakage process inside the pipeline under a near-adiabatic condition.

The leakage behaviour of the supercritical CO₂ includes the jet dispersion outside the pipeline and the variation of the CO₂ flow inside the pipeline [22]. A test section is settled in the main pipeline section to record the characteristic data of the highly pressurised CO₂ inside the pipeline during the leakage process, which is shown in Fig. 2.

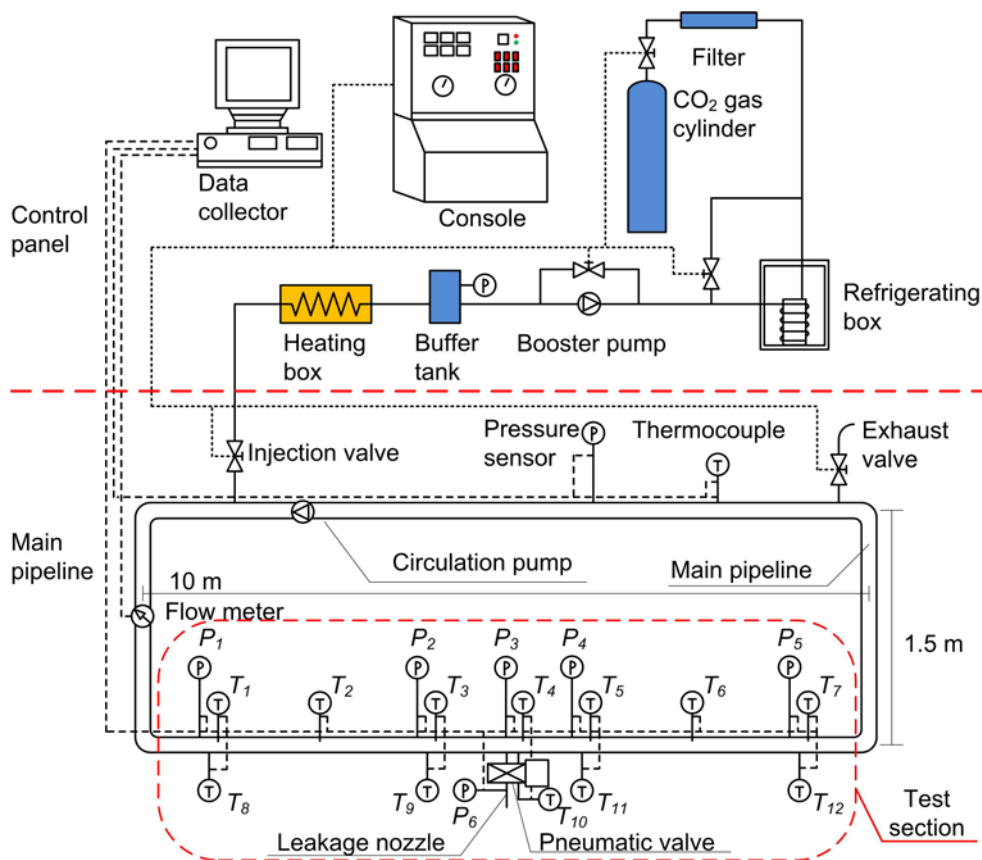


Fig. 2. Schematic of the test section.

In the experiments, 12 armored thermocouples were mounted at 7 different positions along the pipeline with measurement accuracy of $\pm 0.25\%$. T1~T7 record the temperature of CO₂ inside the pipeline and T8~T12 record the temperature of tube wall. 5 pressure sensors are mounted along the tube, while P6 is mounted at the leakage nozzle to obtain the outlet pressure of the CO₂ in the leakage process. The leakage nozzle used which is fitted in the

middle of the test section and controlled by a high pressure pneumatic valve could be dismantled easily to alter for another nozzle design.

For the purpose of investigating the CO₂ outside the pipeline, a series of measurements were taken in the test section. The details of the measurements and a brief diagram of the structure of CO₂ outflow are shown in Fig. 3.

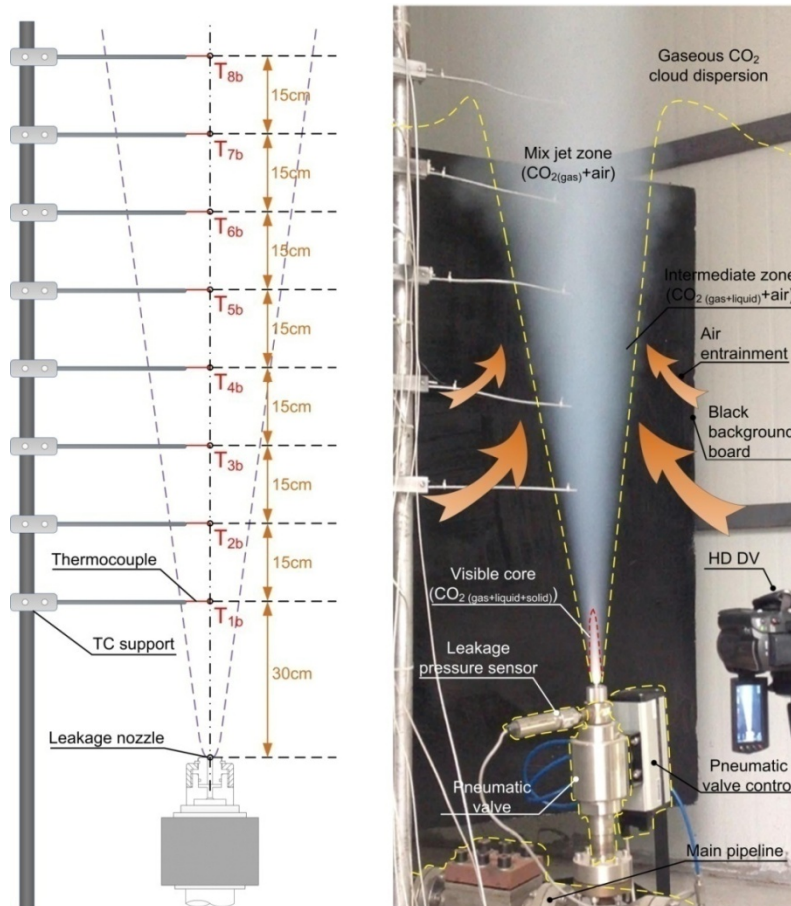


Fig. 3. The details of the measurements and a schematic of the structure of CO₂ outflow.

As shown in Fig. 3, 8 thermocouples are mounted upside the leakage nozzle to obtain the temperature of CO₂ after leakage in the centreline of the jet flow. Two commercial HD DVs (High definition digital videos) with 30 frames per second and a resolution of 1080 p are used to record the information of visible jet plume and development of the dry ice bank.

2.2. Experiment procedure

In the experiments, the CO₂ was pressurised to 9 MPa and then kept circulating in the main pipeline in which the discharge coefficients at the leakage nozzle change with the depressurization significantly [23]. When the measuring devices were ready to record, the injection valve and the heat band would be shut down to maintain the whole leakage process under near-adiabatic and iso-volumetric conditions. Tests would be stopped when the pipeline inner pressure decreased to 1 MPa, and each test was repeated several times to ensure repeatable results within the permitted error range. All measurements were carried out under similar ambient temperature and humidity (55±5 %). The operation conditions are summarized in Table 1.

Table 1

Operating condition in the experiment

Nozzle (RHP)	Initial pressure (MPa)	HD DV	Test section record	Thermocouples outside the pipeline	Temperature (°C)
0.003	9.02	√	×	×	Ambient air
0.017	9.00	√	√	√	20±3
0.030	9.04	√	√	√	Initial CO ₂ in
0.063	9.01	√	√	√	pipeline
0.082	9.04	√	√	√	40±1

3. Results and discussion

According to the typical jet release model used in the analysis of the accidental release, the leakage process of supercritical CO₂ could be separated into four regions: source region, jet dispersion, vapor cloud dispersion, and dry ice bank [24]. In the experiments, the thermocouples and HD-DVs which were mounted outside the leakage nozzle recorded the phenomena of jet dispersion, the development of dry ice bank and the temperature in the centreline of the jet plume. Thermocouples and pressure sensors mounted in the test section were used to obtain the variation of the temperature and pressure of CO₂ in the source region.

3.1. Jet dispersion phenomena

In the accidental release, highly pressurised CO₂ decompresses rapidly outside the leakage nozzle and experiences an explosive expansion, leading to a typical under-expanded plume in the dispersion process, which could be seen clearly as a white plume in the experiments. The jet dispersion at different leakage nozzles was observed and the results are shown in Fig. 4.

Initial pressure=9 MPa Leakage time= 1 sec.

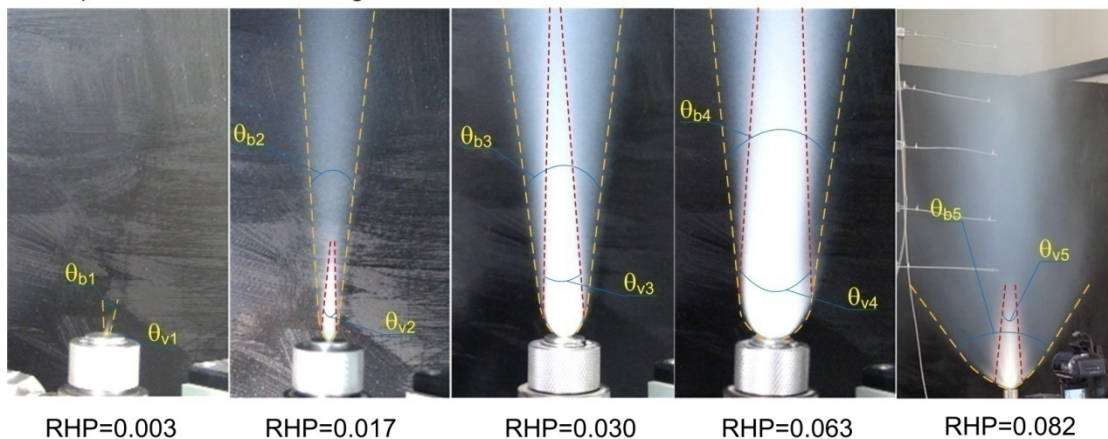


Fig. 4. Jet flow with different leakage nozzles.

The expanded CO₂ in the leakage results in a violent temperature drop of CO₂ fluid itself and the surrounding air, which is known as Joule-Thomson effect (J-T effect). Inside the jet dispersion, an extremely low temperature leads to a phase change of CO₂ from supercritical phase to solid phase. In the central area of the white plume, a white visible core is formed and then weakened away from the leakage nozzle. In the experiments, the extent of the barrel expansion at the bottom of the jet and the boundary of the jet flow could be measured by the divergent angle of the jet boundary. In order to describe the influence and ranges of the white visible core, the convergent angles at the top of the core were obtained. The divergent angle of the jet flow boundary θ_b and the convergent angle of visible core θ_v at different leakage nozzles are indicatively shown in Fig. 5.

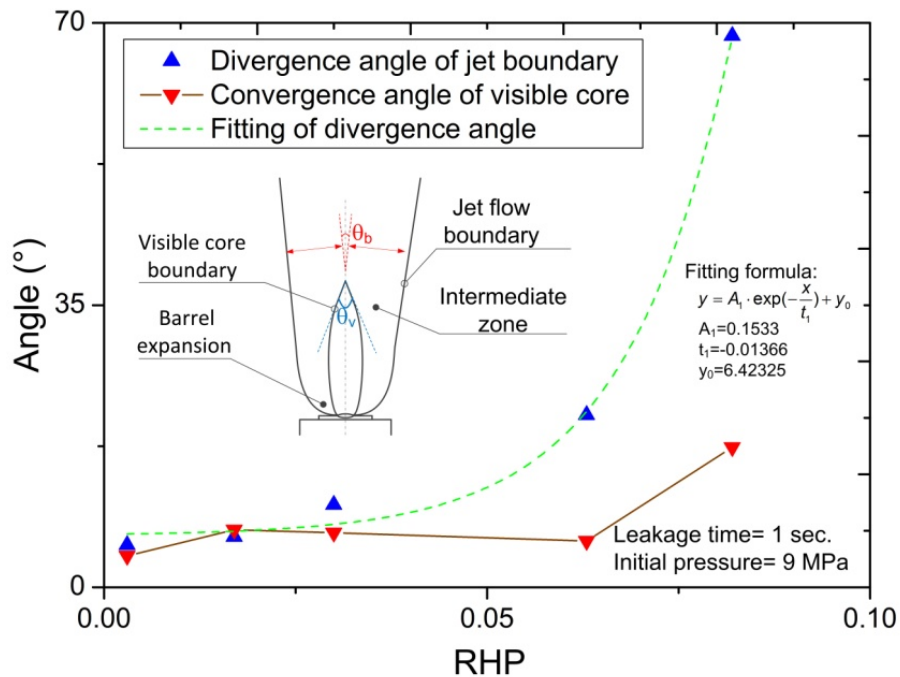


Fig. 5. Convergent angle of the visible core and divergent angle of the jet flow boundary.

It is obvious that the convergent angle of the visible core and the divergent angle of the jet boundary increase with increased size of the leakage nozzle, meanwhile the divergent angle changes rapidly and could be fitted mathematically by a logarithmic function.

3.2. Dry ice bank

Due to the violent temperature drop caused by J-T effect outside the leakage nozzle, the high density CO₂ around would experience a rapid phase change at the bottom of the jet plume. To evaluate the phase change appeared in the leakage process, temperatures in the jet central line (representing the minimum temperatures in different jet cross-sections) of the jet flow with different leakage nozzles were measured and are shown in Fig. 6.

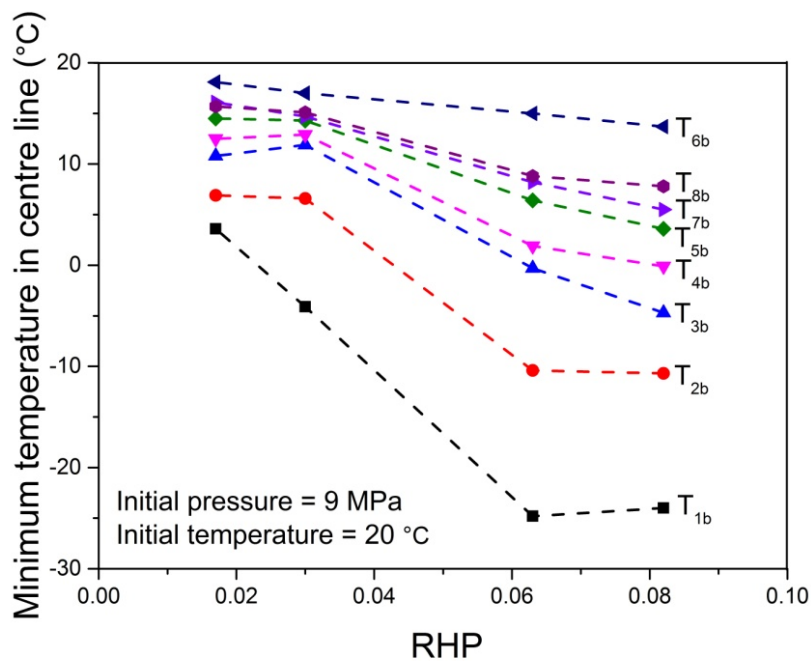


Fig. 6. Minimum temperature in the centreline of the jet flow.

The temperature at T_{1b} which is mounted 30 cm above the leakage nozzle is lower than 0 °C when RHP > 0.02, while the temperature at the leakage nozzle is expected to be much lower.

Carbon dioxide has no liquid state at pressures below 520 kPa. At atmospheric pressure, the gas deposits directly to a solid state called dry ice at temperatures below $-78.5\text{ }^{\circ}\text{C}$ and the solid sublimates directly to a gas above $-78.5\text{ }^{\circ}\text{C}$. However, the leakage flow here is quite complex: the leaked CO_2 mixed with the ambient air immediately after the nozzle exit and the temperatures measured in the experiments were for the CO_2 -air mixtures in a highly under-expanded transient flow some distances about the nozzle exit. The CO_2 near the leakage could probably be capable of changing into solid phase. With the weakening of the jet plume, a flimsy dry ice bank near the jet nozzle exit can be observed clearly and is shown in Fig. 7.

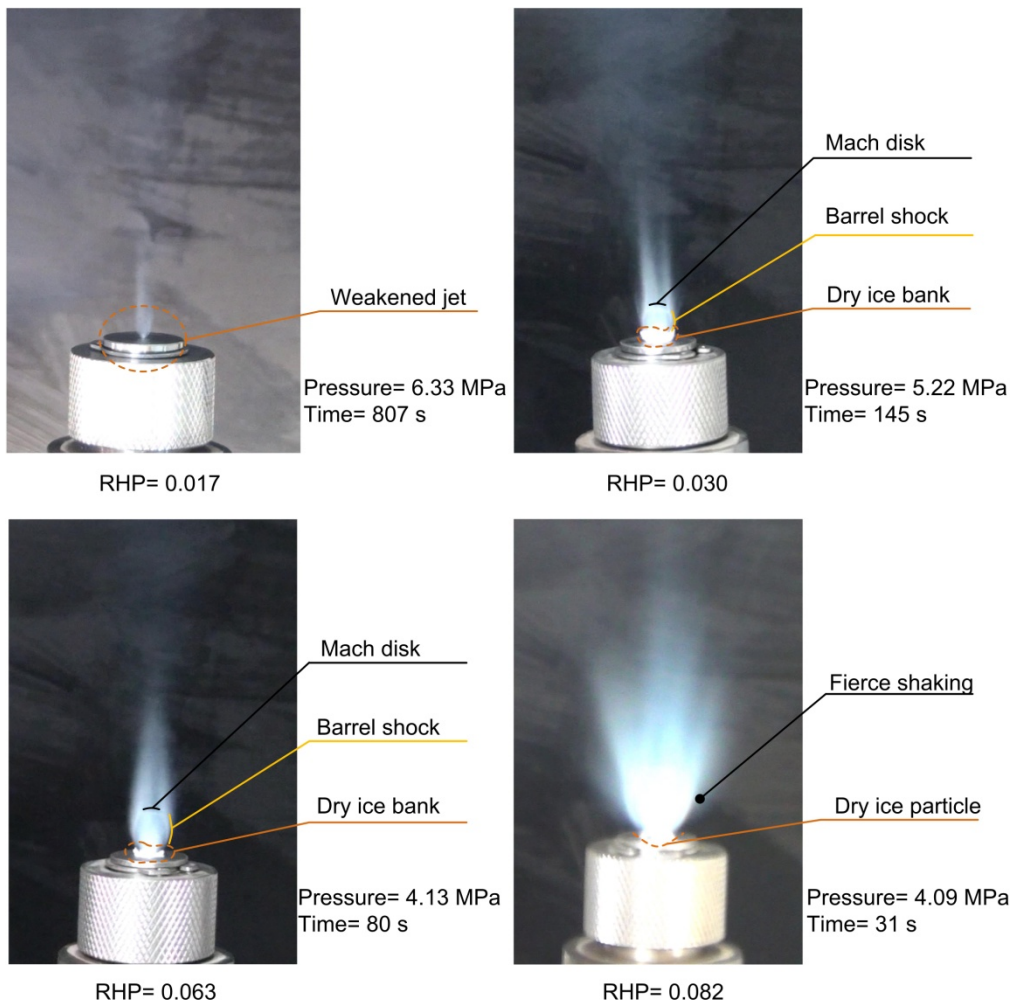


Fig. 7. Dry ice bank.

With different sizes of the leakage nozzles, the jet plume weakened at different inner pressure and the nozzle size had a quite different influence on the development of the dry ice bank. Dry ice particles are almost indistinguishable for small leakage nozzles (small holes) as the temperature could hardly drop below the freezing point of CO₂. When the leakage hole is rather large, the dry ice particles could not accumulate into a steady dry ice bank as the leakage nozzle is shaking fiercely. With the weakening of the jet plume, the particles appeared at the bottom of the plume had the capability of forming dry ice bank for nozzles with medium-sized holes. The Mach disk and barrel shock could also be observed which indicate the variation of the velocity in the jet dispersion.

3.3. *Pressure variations and Mach numbers*

Calculation of the mass outflow rate is the first step of the analysis of the accidental release from damaged pipeline; therefore the Mach number and variation of the pressure were investigated in the experiments to study the flow field at the leakage nozzle. During the experiment, the circulating system was kept at a constant volume; the velocity of the CO₂ outflow at leakage nozzle could be obtained indirectly by the mass outflow rate at the leakage nozzle. The variations of the pressure were obtained from the pressure sensor at the leakage nozzle; meanwhile Mach number could be obtained by calculating the ratio of velocity of CO₂ at leakage nozzle to the local sound speed of the CO₂. As pressure of the CO₂ keeps falling in the leakage process, the free jet would change from sonic flow to subsonic flow at the critical pressure where the velocity of the jet equals to the local sound speed of the CO₂. The results are shown in Fig. 8.

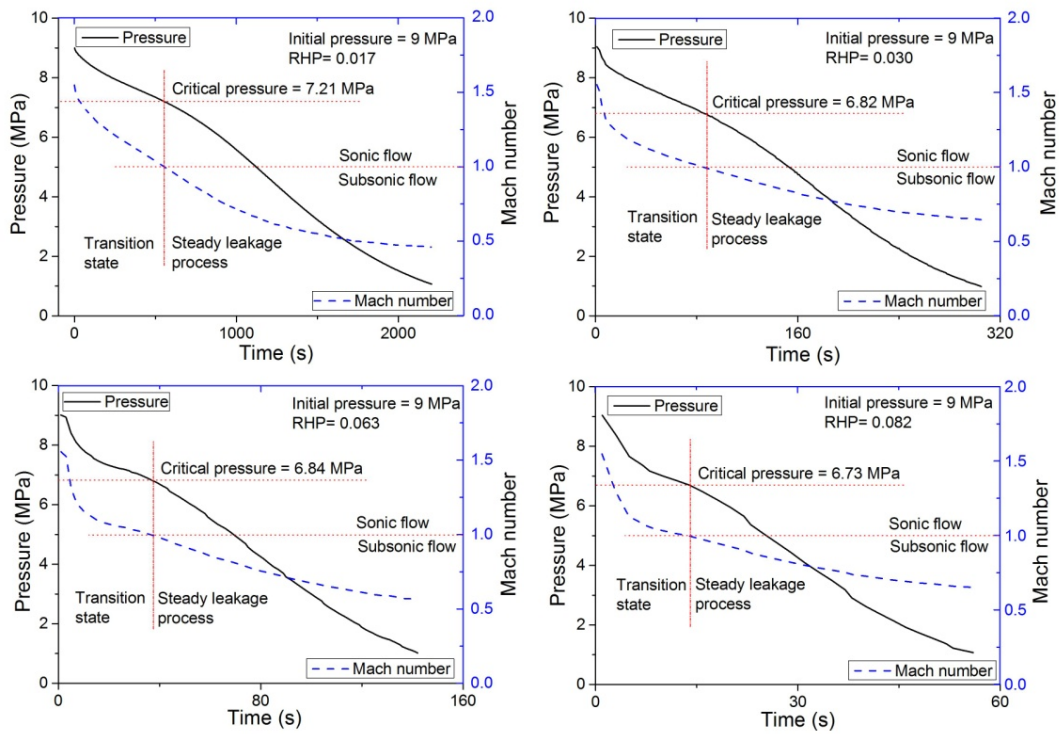


Fig. 8. The variation of pressure and Mach number at the leakage nozzle locations.

The outflow from the leakage nozzle would transform from sonic flow to subsonic flow when the Mach number of the CO₂ flow drops below 1. Consequently the depressurization process could be approximately divided into two stages: the supersonic transitional stage ($Ma > 1$) and steady leakage process ($Ma < 1$). The pressure drops quickly in the supersonic transitional stage (indicated as the “transition state” in Fig. 8), as the choked flow inside the leakage nozzle has a significant influence on the CO₂ flow through the leakage nozzle. While the Mach number drops below 1, the CO₂ flow turns into steady leakage and the gradient of the depressurization process remains more or less a constant. Generally the depressurization process and Mach number at different leakage sizes have similar trends in the leakage process. The critical pressure ($Ma=1$) in depressurization process ranges from 7.20 MPa to 6.73 MPa at different leakage nozzle sizes.

3.4. Local Nusselt number

In the source region of the leakage flow, supercritical CO₂ is choked at the nozzle and experiences a phase change from supercritical phase to co-existing gas-supercritical multiphase during the leakage. The strength of the multiphase choked flow could be measured by the velocity gradient at the leakage nozzle. As the velocity gradient develops with the thermal boundary layer, the local Nusselt number which represents the gradient of the thermal boundary layer (related to the leakage nozzle size) could be used as an indirect parameter for measuring the characteristics of the multiphase choked flow at leakage [25]. Four test points T1, T3, T5 and T7 were setup to record the local Nusselt numbers along the pipeline where T3 recorded the local Nusselt number at the leakage nozzle. As the multiphase choked flow occurs at the leakage nozzle, the local Nusselt number measured at leakage nozzle is much larger than the other test points along the pipeline [22]. In the experiment, the local Nusselt number at the leakage nozzle is chosen for comparison between the different leakage nozzles. The local Nusselt number could be calculated from the local heat transfer coefficient using the formula given as follows:

$$Nu_x = \frac{h_x \cdot D}{\lambda} \quad (3)$$

where D is the internal diameter and λ is the thermal conductivity of CO₂ at the measuring temperature, Nu_x represents the local Nusselt number. A simplified method is used to calculate the local heat transfer coefficient h_x as shown below:

$$h_x = \frac{q_e''}{T_w - T_{in}} \quad (4)$$

where q_e'' is the heat flux, T_w is the inner wall temperature of the pipe which represents the boundary temperature of the thermal boundary layer, and T_{in} is the CO₂ temperature inside the tube which represents the temperature of the fluid.

As the pipe is insulated from the external environment in the experiment, the heat flux associated with the heat convection between the tube and the CO₂ flow can be calculated by the heat loss of the steel tube. The heat flux is calculated by the formula below:

$$\dot{q}_e = c_{V, \text{stl}} \cdot \rho_{\text{stl}} \cdot \delta_{\text{stl}} \cdot \frac{dT_e}{A_e \cdot dt} \quad (5)$$

where $c_{V, \text{stl}}$ is the constant volume heat capacity of the steel in the experiment, ρ_{stl} is the density of the steel, T_e is the temperature of the steel tube in the experiment which can be regarded as uniform as the Biot number is very small in this case, t is the time in the leakage process, S is the inner surface area of the tube, δ_{stl} is the volume of the steel tube. The local Nusselt numbers at the leakage nozzles during the leakage processes are shown in Fig. 9.

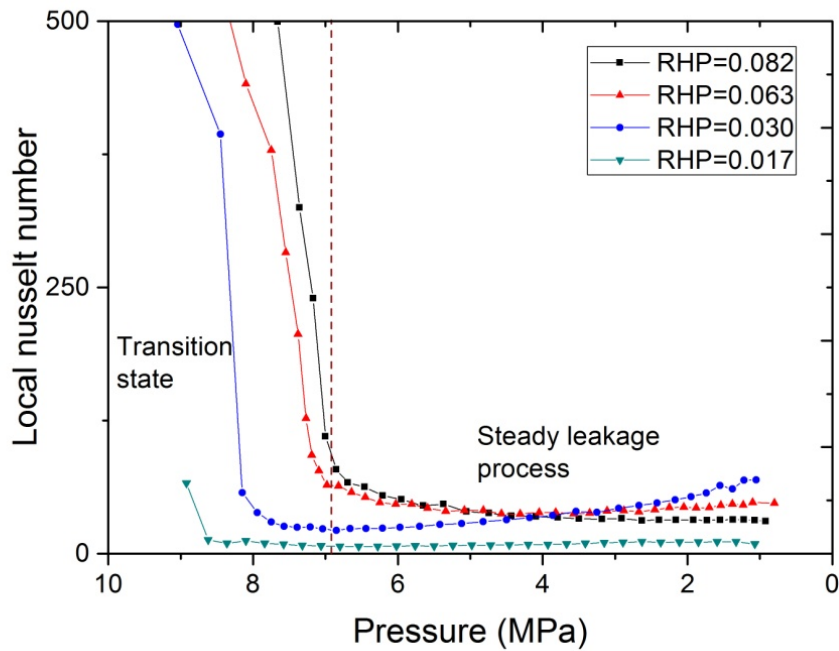


Fig. 9. Variation of local Nusselt number at different leakage sizes.

The local Nusselt numbers of different leakage sizes have a similar trend of variation which decreases rapidly in the transition state of the leakage. The formation of this trend is due to the similar depressurization process in the leakage, as the thermal boundary layer changes with the flow field from a single-phase sonic flow in the beginning of the leakage to a multiphase subsonic flow in the steady leakage process. Then the local Nusselt numbers reach a nearly steady state with a small increase where the variations are no longer significant in the steady leakage process. The average local Nusselt number in the steady leakage process was obtained and shown in Fig. 10.

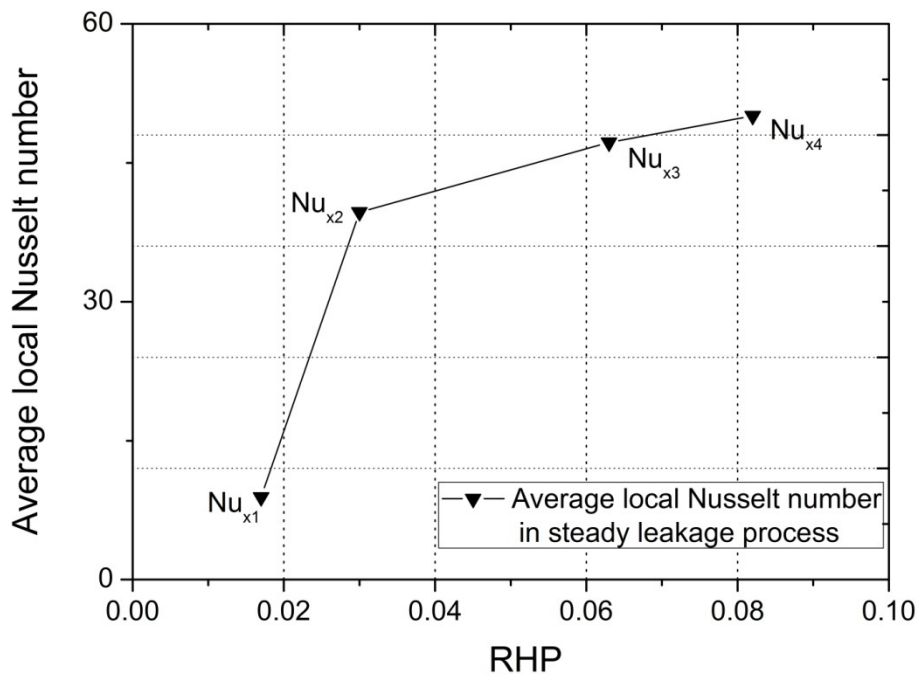


Fig. 10. The average local Nusselt number in the steady leakage process.

The average local Nusselt numbers Nu_x under the four situations in the experiments are 50.06, 47.19, 39.66 and 8.90, respectively. As the local Nusselt number increases with the increasing size of the leakage hole, a thicker thermal boundary layer was formed representing enhanced convective heat transfer. The results indicate that multiphase choked

flow at the leakage nozzle strengthens when the leakage hole size is increased and weakens for small holes.

3.5. *Accidental release model and mass outflow rate*

For the purpose of comparing and analysing the mass outflow rate from the experimental study, several accidental release models are used. As significant variations exist in fluid density during the typical accidental release process, the CO₂ flow in the pipeline is considered as highly compressible at leakage conditions. In the leakage process, there are significant variations in pressure, temperature and density. In order to analyze the accidental release flow system, four main equations are considered: the equations of the state, continuity, momentum and energy. Meanwhile the process is assumed to be reversible (which will be far from the reality) and adiabatic to simplify the analysis. Generally two situations are concerned for the gas release: (a) gas flow through a hole with the pipeline considered as a tank: usually called the “hole model”; (b) gas flow through the completely ruptured pipeline: the “pipe model”. However there is a major gap between these two models: all the cases ranging from a “pinhole” to a “rupture” (the “hole model” could be applied to “pinhole” while the “pipe model” could be used for full rupture of the pipe). A “modified model” was proposed to bridge up this gap [16]. In the “modified model”, different simplifications are used depending on whether the flow is sonic. In practice, if accidental release is detected, the valves at both sides of the pipe would shut down immediately. The flowing CO₂ can be considered as satisfying situation (a) and the whole leakage process is iso-volumetric so that the pipeline could be considered as a tank. Therefore the “hole model” and “modified model” could both be applicable for the accidental release for the small leakage hole. In the following, both accidental release models are introduced and mass outflow rates are calculated in comparison with the experimental data.

3.5.1. The hole model

A schematic diagram of the accidental release system is given by Helena et al [16] which is shown in Fig. 11.

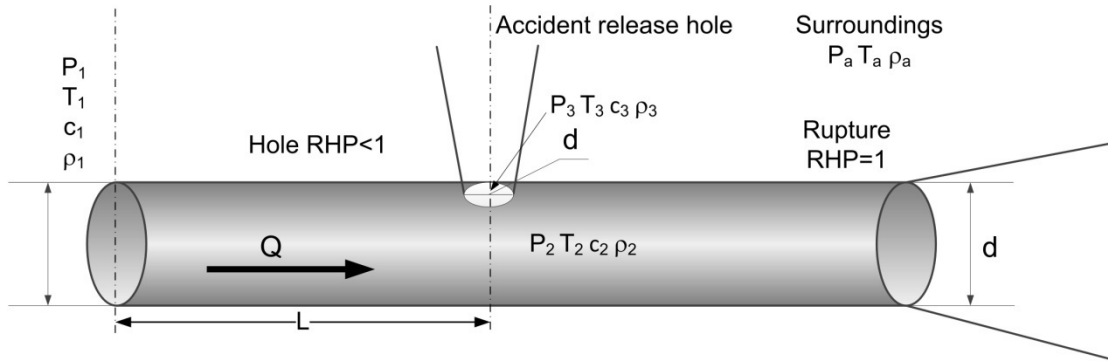


Fig. 11. Schematic diagram of accidental release system.

The accidental release hole is located at a distance L from the pipeline starting point 1, while point 2 is inside the pipeline at the location of the hole and point 3 is the leakage point.

Applying the equations of energy and momentum to the adiabatic flow of CO_2 in the pipeline, the following equation [16] is obtained:

$$\frac{k+1}{k} \cdot \ln\left(\frac{P_1 \cdot T_2}{P_2 \cdot T_1}\right) + \frac{M}{RG^2} \cdot \left(\frac{P_2^2}{T_2} - \frac{P_1^2}{T_1}\right) + \frac{4fL_e}{D} = 0 \quad (6)$$

where L_e is the equivalent length of the pipeline, f is the friction factor which is a function of the roughness of the pipe and the Reynolds number, and G is the mass flux.

Assuming the expansion outside the leakage is an isentropic and quasi-static process, substituting continuity equation and the state equation for real gas in Eq. (3), the mass outflow rate Q could be calculated by the formula [16] below:

$$Q = C_0 \cdot S \cdot P_2 \sqrt{\frac{2M}{ZRT_2} \cdot \frac{k}{k-1} \cdot \left[\left(\frac{P_a}{P_2}\right)^{\frac{2}{k}} - \left(\frac{P_a}{P_2}\right)^{\frac{k+1}{k}} \right]} \quad (7)$$

where C_0 is empirical discharge coefficient, S is the area of the leakage hole, Z is the compressibility factor. Generally, the pressure of the surrounding is the atmospheric pressure and the mass outflow rate is determined by the pressure and temperature of CO_2 at the leakage nozzle.

3.5.2. The modified model

A modified model was proposed to bridge the gap between the “hole model” and “pipe model” [19, 20]. To calculate the mass outflow rate from leakage in this “modified model”, whether the flow through the leakage hole is sonic should be considered as the initial condition. Critical pressure ratio (CPR) is widely used to decide whether the leakage is sonic or subsonic in theoretical analysis; whereas it is difficult to obtain in an experimental investigation. Firstly the sound velocity of CO_2 at leakage point needs to be determined, which could be calculated through the real gas state equation as follows:

$$v_s = \sqrt{\frac{ZRT_2}{M} \cdot k} \quad (8)$$

and then the maximum speed of the CO_2 at leakage nozzle could be obtained from the energy equation under an isentropic condition:

$$v_m = \sqrt{2c_p \cdot (T^* - T_a)} \quad (9)$$

where c_p is the constant-pressure specific heat capacity, T^* is the stagnation temperature which equals to the initial static temperature before the expansion at leakage. Mach number in the experimental investigation is defined as:

$$Ma = v_m / v_s \quad (10)$$

when the Mach number (Ma) is larger than unity, the flow at the nozzle is sonic, the mass outflow rate could be obtained from the formula [19] below:

$$Q = C_0 \cdot S \cdot P_2 \sqrt{\frac{M}{ZRT_2} \cdot k \cdot \left[\frac{2}{k+1} \right]^{\frac{k+1}{k-1}}} \quad (11)$$

when the outflow is subsonic as $Ma < 1$, the mass flow rate is given via Eq. (4). Generally the mass outflow rate calculated in the “modified model” depends on the Mach number. The Mach numbers at different leakage sizes during the leakage process are obtained as shown above. Then the mass outflow rate could be calculated using the “modified model”.

3.5.3. Mass outflow rate

The mass outflow rate of CO_2 is obtained through calculation of the reduction of the mass of CO_2 inside the pipeline along the depressurization process. In the experiment, the main pipeline part was kept at a constant volume. The mass of CO_2 inside the pipeline can be calculated by the formula below:

$$m_{CO_2} = \rho_{CO_2} \times V_{CO_2} \quad (12)$$

where ρ_{CO_2} denotes the density of the CO_2 which varies with the pressure and temperature inside the pipeline, V_{CO_2} denotes the volume of the CO_2 inside the pipeline. The mass outflow rate is the time derivative of the mass of the CO_2 inside the pipeline in the experiment.

Comparing with the data calculated from the “hole model” and “modified model”, the mass outflow rates of CO_2 are shown in Fig. 12.

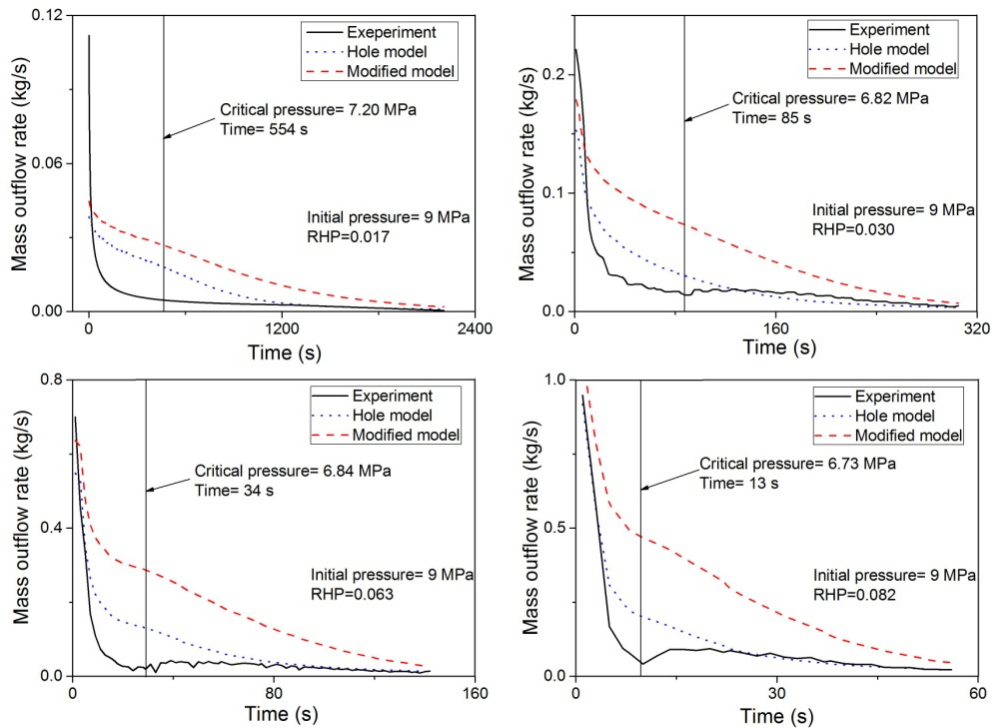


Fig. 12. Mass outflow rate in the experiment and the calculation results from the “hole model” and “modified model”.

The results show that the mass outflow rate calculated by the “hole model” is closer to the experiment data although both of them over-predict the experimental data in general. The two models also behave differently, leading to large differences in their predictions when the hole size is larger than a small hole $RHP > 0.02$. Overall, the “modified model” significantly overestimates the mass outflow rate from the nozzle hole, especially for larger hole sizes. Although both models are able to predict the initial sudden drop of the mass outflow rate, their predictions are rather poor at the later stages of the transient leakage process. It is also noticed that the “hole model” agrees better with the experiment data in the steady leakage process than the “modified model”. The discrepancies observed between the experimental data and model predictions can be mainly attributed to the model assumptions such as the reversible flow assumption for the leakage process. A significant amount of

efforts are called for the development of high-fidelity theoretical models for the high pressure leakage process.

4. Concluding remarks

Experiments to investigate the supercritical CO₂ leakage behaviour with different leakage nozzle sizes have been conducted. The pressure and Mach number in the depressurization process and the local Nusselt number were obtained. Meanwhile a comparison of mass outflow rate between experiments and typical release models has been carried out. In the measurements, the accuracy and the repeatability of the data were verified by a series of repeatable experimental tests. According to the results and analysis, some conclusions are summarised as follows:

- (1). The typical jet plume structures outside the leakage nozzle at different nozzle sizes were observed and the divergent angle of the jet boundary increases rapidly with the increase of the size of the leakage hole.
- (2). The temperatures in the centreline of jet flow were obtained showing that dry ice bank could only appear for leakage holes of medium size with steady leakage flows.
- (3). The Mach number and variation of the pressure at the leakage nozzle were obtained indicating that the supercritical CO₂ at the leakage nozzle changes from sonic leakage into subsonic leakage during the depressurization process.
- (4). The local Nusselt numbers were obtained, which indicate that the convective heat transfer of the multiphase flow inside the leakage nozzle is enhanced with increased leakage nozzle size and changes insignificantly in the steady leakage process when the inner pressure drops below the critical pressure.
- (5). The mass outflow rates in the experiments were obtained and compared with the results from typical accidental release models. The mass outflow rate calculated from

the “hole model” agrees better with the experiment data than the “modified model” for small leakage holes.

Further studies including the Reynolds number of the leakage flow, influence of the initial pressure and impurities, the acoustic fields and vibrations of the pipeline associated with the leakage process, as well as numerical modelling research are currently underway.

Acknowledgments

This work was supported by the Thousand Talent Program of China and China Postdoctoral Foundation (Project No. 2012M521253). The authors thankfully acknowledge all these supports.

References

- [1] Bowen F. Barriers to carbon capture and storage may not be obvious. *Nature* 464 (2010) 160.
- [2] Haszeldine RS. Carbon Capture and Storage: How Green Can Black Be? *Science* 325 (2009) 1647-52.
- [3] Robert H. Socolow. Can we bury global warming? *Sci Am* 293 (2005) 49-55.
- [4] Schrag DP. Preparing to Capture Carbon. *Science* 315 (2007) 812-3.
- [5] Jiang X, Akber Hassan WA, Gluyas J. Modelling and monitoring of geological carbon storage: A perspective on cross-validation. *Applied Energy* 112 (2013) 784-92.
- [6] Aspelund A, Jordal K. Gas conditioning—The interface between CO₂ capture and transport. *International Journal of Greenhouse Gas Control* 1 (2007) 343-54.

- [7] Svensson R, Odenberger M, Johnsson F, Strömberg L. Transportation systems for CO₂—application to carbon capture and storage. *Energy Conversion and Management* 45 (2004) 2343-53.
- [8] World Resources Institute (WRI). CCS guidelines: guidelines for carbon dioxide capture, transport, and storage. Washington, DC.: World Resources Institute.2008.
- [9] Joana S, Joris M, Evangelos T. Technical and economical characteristics of CO₂ transmission pipeline infrastructure. Technical report, JRC Scientific and Technical Reports, European Commission. 2011.
- [10] Working Group III of the Intergovernmental Panel on Climate Change [Metz B, O. Davidson, H.C. de Coninck, M. Loos, and L.A. Meyer (eds.)]. Special Report on Carbon Dioxide Capture and Storage. Cambridge University Press, Cambridge, United Kingdom and New York, NY, USA,,: IPCC; 2005, pp. 442.
- [11] McCoy ST, Rubin ES. An engineering-economic model of pipeline transport of CO₂ with application to carbon capture and storage. *International Journal of Greenhouse Gas Control* 2 (2008) 219-29.
- [12] International Energy Agency Greenhouse Gas R&D Programme. CO₂ storage in depleted gas fields. Technical Study Report 2009 No.2009/01.
- [13] Skovholt O. CO₂ transportation system. *Energy Conversion and Management* 34 (1993) 1095-103.
- [14] Molag M, Dam C. Modelling of accidental releases from a high pressure CO₂

- pipelines. *Energy Procedia* 4 (2011) 2301-7.
- [15] Tu R, Xie Q, Yi J, Li K, Zhou X, Jiang X. An experimental study on the leakage process of high pressure CO₂ from a pipeline transport system. *Greenhouse Gases: Science and Technology* 4 (2014) 777-784.
- [16] Montiel H, Vílchez JA, Casal J, Arnaldos J. Mathematical modelling of accidental gas releases. *Journal of Hazardous Materials* 59 (1998) 211-33.
- [17] 8th Report of the European Gas Pipeline Incident Data Group. 8th EGIG report. EGIG; 2011. pp. 43.
- [18] Carter DA. Aspects of risk assessment for hazardous pipelines containing flammable substances. *Journal of Loss Prevention in the Process Industries* 4 (1991) 68-72.
- [19] Dong Y, Gao H, Zhou J, Feng Y. Mathematical modeling of gas release through holes in pipelines. *Chemical Engineering Journal* 92 (2003) 237-41.
- [20] Dong Y, Gao H, Zhou J, Feng Y. Evaluation of gas release rate through holes in pipelines. *Journal of Loss Prevention in the Process Industries* 15 (2002) 423-8.
- [21] Xie Q, Tu R, Jiang X, Li K and Zhou X. The leakage behavior of supercritical CO₂ flow in an experimental pipeline system. *Applied Energy* 130 (2014) 574-580.
- [22] Li K, Zhou X, Tu R, Xie Q, Jiang X. The flow and heat transfer characteristic of supercritical CO₂ leakage from a pipeline. *Energy* 71 (2014) 665-672.
- [23] Edlebeck J, Nellis GF, Klein SA, Anderson MH, Wolf M. Measurements of the flow

of supercritical carbon dioxide through short orifices. The Journal of Supercritical Fluids 88 (2014) 17-25.

[24] Bricard P, Friedel L. Two-phase jet dispersion. Journal of Hazardous Materials 59 (1998) 287-310.

[25] Zhang X-R, Yamaguchi H. An experimental study on heat transfer of CO₂ solid–gas two phase flow with dry ice sublimation. International Journal of Thermal Sciences 50 (2011) 2228-34.